THE JOURNAL OF BIOLOGICAL CHEMISTRY VOL. 286, NO. 47, pp. 40792–40801, November 25, 2011


# Deciphering the Xcp *Pseudomonas aeruginosa* Type II Secretion Machinery through Multiple Interactions with Substrates*[S]◆

Received for publication, August 18, 2011, and in revised form, September 23, 2011 Published, JBC Papers in Press, September 26, 2011, DOI 10.1074/jbc.M111.294843

**Badreddine Douzi**[‡§], **Geneviève Ball**[‡], **Christian Cambillau**[§], **Mariella Tegoni**[§1], **and Romé Voulhoux**[‡2]

*From the* [‡]*Laboratoire d'Ingénierie des Systèmes Macromoléculaires (LISM-UPR9027), Institut de Microbiologie de la Méditerranée, CNRS, Aix-Marseille Université, 31 Chemin Joseph Aiguier, 13402 Marseille cedex 20 and the* [§]*Architecture et Fonction des Macromolécules Biologiques (AFMB-UMR6098), CNRS, Aix-Marseille Université, Case 932, 163 Avenue de Luminy, 13288 Marseille cedex 9, France*

**Background:** The type II secretion machinery secretes large toxins across the bacterial envelope.
**Results:** We identified multiple interactions between secreted exoproteins and components of the machinery.
**Conclusion:** We propose a model for substrate recognition and transport during the secretion process.
**Significance:** Our data shed light on the operating mode of the type II secretion pathway and provide new potential targets for drug development.

**The type II secretion system enables Gram-negative bacteria to secrete exoproteins into the extracellular milieu. We performed biophysical and biochemical experiments to identify systematic interactions between *Pseudomonas aeruginosa* Xcp type II secretion system components and their substrates. We observed that three Xcp components, $XcpP_C$, the secretin $XcpQ_D$, and the pseudopilus tip, directly and specifically interact with secreted exoproteins. We established that $XcpP_C$, in addition to its interaction with the substrate, likely shields the entire periplasmic portion of the secreton. It can therefore be considered as the recruiter of the machinery. Moreover, the direct interaction observed between the substrate and the pseudopilus tip validates the piston model hypothesis, in which the pseudopilus pushes the substrate through the secretin pore during the secretion process. All together, our results allowed us to propose a model of the different consecutive steps followed by the substrate during the type II secretion process.**

Gram-negative bacteria have evolved different sophisticated secretory machines specialized for the secretion of specific categories of exoproteins (1). The type II secretion pathway is widely used by many Gram-negative bacteria for the secretion of major virulence factors in plants and animals (2). In this two-step secretion process, proteins are synthesized with a cleavable N-terminal signal sequence that enables their transport across the cytoplasmic membrane by the Sec or Tat general export machinery (3). After acquisition of their folds in the periplasm, type II secretion-dependent proteins are specifically recognized and loaded by a large macromolecular machine, the secreton, for their final release into the external milieu. The secreton spans the entire bacterial envelope and consists of at least 12 different Gsp proteins that are organized in three subcomplexes depending on their cellular localizations and mutual interactions (4).

The $GspE_R$, $F_S$, $L_Y$, and $M_L$ proteins (see "Experimental Procedures" for nomenclature) form the inner membrane (IM)[3] platform, where the $GspE_R$ traffic ATPase provides energy for the system (5–8). The second subcomplex is called the pseudopilus, which is analogous to the pilus structure found in the type IV piliation system. The pseudopilus consists of five pseudopilins, all of which are subjected to maturation by the prepilin peptidase $GspO_A$, which is also involved in the maturation of the type IV pilins. The pseudopilus is formed by the helical assembly of the major pseudopilin $GspG_T$ (9), and it has a quaternary complex of the four minor pseudopilins at its tip (10, 11). This structural similarity to the type IV piliation system suggests that the pseudopilus might also assemble on the IM platform in a pilus-like structure to push the substrate like a piston through the third subcomplex of the secreton, the secretin $GspD_Q$ (10–14).

Secretins form large, homo-multimeric pores in the outer membrane (OM). They are components of various secretion or assembly machines involved in the transport of large structures (15). Each secretin monomer has two domains: the conserved C-terminal domain, which forms the pore in the OM, and the N-terminal domain, which differs between transport systems and forms an extension of the pore cavity in the periplasm. The N-terminal domains of T2SS secretins consist of four structurally independent subdomains named N0 to N3 from the N to the C terminus. Recently, Reichow *et al.* (12) have reported direct interactions between $GspD_Q$ and the substrate and

* This work was supported by "3D-Pilus" Young Researcher Agence Nationale de Recherches (ANR) Grant ANR-JC07-183230.
◆ This article was selected as a Paper of the Week.
[S] The on-line version of this article (available at http://www.jbc.org) contains supplemental experimental procedures and Tables S1 and S2.
[1] To whom correspondence may be addressed. Tel.: 33-4-91-82-55-92; Fax: 33-4-91-26-67-20; E-mail: mariella.tegoni@afmb.univ-mrs.fr.
[2] To whom correspondence may be addressed. Tel.: 33-4-91-16-41-26; Fax: 33-4-91-71-21-24; E-mail: voulhoux@ifr88.cnrs-mrs.fr.

[3] The abbreviations used are: IM, inner membrane; OM, outer membrane; T2SS, type II secretion system; MALS, multiangle light scattering; QELS, quasi-elastic light scatter detection; HR, homology region; TMHR, transmembrane homology region; RU, response unit.

between $GspD_Q$ and the pseudopilus. This important finding agrees with the secreton model, in which the pseudopilus interacts with the secretin containing the substrate to push it through the pore. However, no evidence has been reported in the literature for a direct interaction between the pseudopilus and the substrate.

In different representations of the secreton, the connection between the IM platform and the OM secretin is mediated by $GspC_P$. This component is inserted into the IM platform by its N-terminal transmembrane helix and is connected to the secretin by its periplasmic domain on the other side (16, 17).

T2SSs are prevalent among Gram-negative bacteria and are highly specific for their respective substrates. In *Pseudomonas aeruginosa*, two T2SSs co-exist, Xcp and Hxc, and each secretes a specific set of substrates (18).

In contrast to other secretory machines, such as the type I, type III, and type IV secretion systems, no secretion recognition signals have yet been identified for type II secretion. However, several studies have indicated the involvement of several non-adjacent regions in substrate recognition, thus suggesting the existence of a conformational secretion signal (19, 20).

Notably, no interactions between substrates and secreton components other than the secretin have been reported so far. In this work, we aimed at understanding two critical steps of the type II secretion process, the initial substrate recognition and its release after import inside the machinery. To do this, we set up a systematic protein/protein interaction study between secreted substrates and different periplasmic components of the T2SS secreton. The multiple interactions identified made it possible to propose a model of substrate recruitment and transport during the type II secretion process.

## EXPERIMENTAL PROCEDURES

*Nomenclature Used in This Study*—Because a different nomenclature is used for non-*Pseudomonas* and *Pseudomonas* T2SSs, the alternative gene or protein nomenclature is indicated throughout this study; for example, in $GspE_R$, the "R" refers to XcpR, which is reciprocally called $XcpR_E$. Moreover, all of the $XcpP_C$, $XcpQ_D$, and pseudopilin variants used in this study are periplasm-soluble domains, lacking their membrane domains, and are respectively called $P_C$, $Q_D$ and $T_G$, $U_H$, $V_I$, and $W_J$ and $X_K$ for the pseudopilin variants.

*Cloning, Expression, and Purification of $P_C$, $^{His}P_C$, $Q_D$-$N^{0123}$, $Q_D$-$N^{012}$, and $Q_D$-$N^{01}$ and the Soluble Domains of the Xcp Pseudopilins*—Cloning, expression, and purification of $P_C$, C-terminal His-tagged $P_C$ ($^{his}P_C$), $Q_D$-$N^{0123}$, $Q_D$-$N^{012}$, and $Q_D$-$N^{01}$ followed the strategy used in Ref. 10 for $T_G$, $U_H$, $V_I$, $W_J$, and $X_K$ cloning, expression, and purification and are described in detail in the supplemental material (Tables S1 and S2).

*Exoprotein Preparation*—The purified, folded, and active *P. aeruginosa* elastase (LasB) and lipase (LipA) used in the surface plasmon resonance (SPR) experiments were respectively purchased from Nagase ChemteX Corp., Kyoto, Japan (lot number 6528025) and obtained from Prof. Jaeger, who purified LipA as described in Stuer *et al.* (21). *P. aeruginosa* alkaline phosphatase LapA was purified from the supernatants of 1l cultures of the PAO1Δ*xcp* strain grown under phosphate starvation as described in Ref. 18. Supernatant collected after centrifugation was concentrated and passed through a Sephadex G75 column equilibrated with 50 mM phosphate, 150 mM NaCl, pH 7. Pure LapA was recovered in fractions corresponding to its molecular mass.

*Biotinylation and Immobilization of $P_C$ on Streptavidin Chip*—$P_C$ was biotinylated with Sulfo-NHS-SS-Biotin (Pierce) following the protocol specified by the supplier, with minor modifications. The protein was diluted at 25 mM in 50 mM phosphate buffer ($Na_2HPO_4/NaH_2PO_4$), 150 mM NaCl, pH 7.5, and the reagent was added at 25 mM (molar ratio 1:1). The reaction was allowed to run for 4 h on ice. To eliminate the excess reagent, the protein solution was first filtered on an NAP-5 column (GE Healthcare) equilibrated in the same buffer as specified above and then dialyzed by a Novagen dialyzer midi (cutoff 3.5 kDa) against 2 times 400 ml of the same buffer as specified above, at 4 °C overnight.

The streptavidin chip was used in 50 mM phosphate buffer, 150 mM NaCl, pH 7. Washing with 1 M NaCl and 50 mM NaOH was carried out as specified by the supplier before fixing biotinylated $P_C$ (1.25 mM, 140 μl at 10 μl/min) at 1295 Δ response unit (RU). Non-biotinylated LipA, LasB, $U_H$, $V_I$, $W_J$, $T_G$, and $X_K$ in 50 mM phosphate, 150 mM NaCl, pH 7 were passed over the two flow cells (10 mM, 60 μl at 10 μl/min) to test for binding. Reproducible interaction was detected with LipA and a high concentration of LasB in the presence of the inhibitor (1–10-phenanthroline (10 mM)). Binding traces were recorded for 5 concentrations of LipA, in triplicate. No regeneration was necessary as spontaneous dissociation of the analyte was observed.

*Immobilization of Antibody Anti-penta-His*—The CM5 sensor chip was coated with the antibody anti-penta-His (Qiagen catalog number 34660) following the procedure in Ref. 22 with minor modifications. Antibody anti-penta-His 50 μg/ml in 10 mM sodium acetate, pH 4.5, was immobilized by amine coupling (ΔRU = 7000) on Fc1 and Fc2. A solution of $^{his}P_C$ at 20 μM in HEPES buffer/EDTA/P20 detergent, pH 7.4, was passed over Fc2 (final ΔRU = 1300). We observed that the amount of fixed $^{his}P_C$ decreases slowly with time (~50% in 3–4 h). To start with a comparable amount of bound ligand, $^{his}P_C$ was fixed at the same level (ΔRU = 1200–1300) before each titration cycle. Solutions of $Q_D$-$N^{0123}$, $Q_D$-$N^{012}$, $Q_D$-$N^{01}$, $T_G$, $X_K$, $U_H$, $V_I$, $W_J$, LipA, LapA, and LasB in the presence of the inhibitor (1–10-phenanthroline 10 mM) and the quaternary complex $U_H$-$W_J$-$V_I$-$X_K$ (20 μM in HBS-EP, pH 7.4, 0.005% P20 detergent) were passed over the Fc2 with $^{his}P_C$ bound and on the control flow cell (Fc1).

*Immobilization of LasB and LapA*—The CM5 (carboxymethylated dextran) sensor chip was coated with LasB and LapA (80 μg/ml in 10 mM sodium acetate, pH 4 and pH 4.5, respectively, for LasB and LapA) immobilized with amine coupling (ΔRU = 800 for LasB and ΔRU = 1500 for LapA) on Fc2. Solutions of $P_C$, $Q_D$-$N^{0123}$, $Q_D$-$N^{012}$, $Q_D$-$N^{01}$, $T_G$, $X_K$, $U_H$, $V_I$, $W_J$, and the quaternary complex $U_H$-$W_J$-$V_I$-$X_K$ (20 μM in HBS-EP, pH 7.4, 0.005% P20) were passed over Fc2 with LasB or LapA bound and on the control flow cell (Fc1). In the case of LasB, reproducible signals were detected with $Q_D$-$N^{0123}$, $Q_D$-$N^{012}$, $Q_D$-$N^{01}$, $X_K$, $U_H$, $V_I$, and the quaternary complex $U_H$-$W_J$-$V_I$-$X_K$; no evidence of interaction has been found with $T_G$ and $W_J$ under the present experimental conditions. When $Q_D$-$N^{0123}$, $Q_D$-$N^{012}$, $Q_D$-$N^{01}$, $X_K$, $U_H$, $V_I$, and the quaternary complex $U_H$-$W_J$-$V_I$-$X_K$ were passed over Fc2 with LapA bound, no interaction

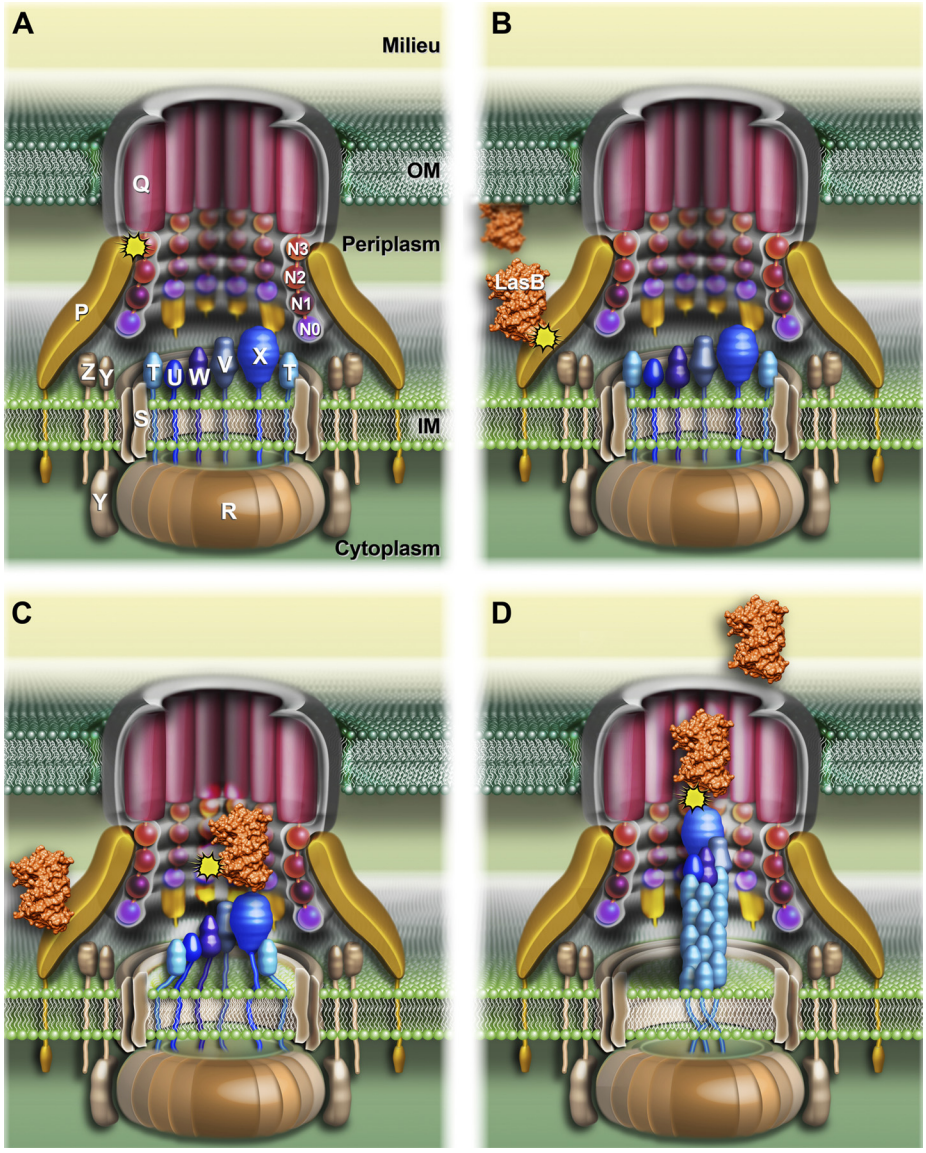


FIGURE 1. **Schematic three-dimensional model of the *P. aeruginosa* Xcp secreton showing substrate recognition and transport during the type II secretion process.** *A*, the schematic representation of the *P. aeruginosa* Xcp secreton. All Xcp components (labeled following Xcp nomenclature only) are represented according to their cellular localization, topology, and multimerization state. *B–D*, the different consecutive steps followed by the substrate for its recruitment, transport, and release by the secreton during the type II secretion process (see "Discussion" for details). The interactions identified in this study are represented by *yellow asterisks*.

was found under the present experimental conditions. Nonspecific binding was subtracted from the binding traces before calculation. Dissociation constants ($K_d$) were estimated based on the equilibrium level at 300 s of injection of LipA on $P_C$ and $P_C$ on LasB and at 175 s of injection of the other combinations.

*Affinity Measurements*—Steady-state analysis of the interactions between soluble domains of $P_C$, $Q_D$-$N^{0123}$, $Q_D$-$N^{012}$, and $Q_D$-$N^{01}$, pseudopilins ($T_G$, $U_H$, $V_I$, $W_J$, and $X_K$), and substrates (LasB, LipA, and LapA) were performed on a BIAcore X100 at 25 °C. All buffers were 0.2 $\mu$m-filtered and degassed before use.

Binding traces were recorded in duplicate for increased concentrations of analyte. In each cycle, $^{his}P_C$ was injected first at reproducible levels of $\Delta RU = 1{,}200-1{,}300$, and the analyte was then injected (40 $\mu$l at 5 $\mu$l/min). Ten millimolar $H_3PO_4$ (2 $\mu$l at 5 $\mu$l/min) was used to regenerate the CM5-anti-penta-His surface. Reproducible signals were detected with $Q_D$-$N^{0123}$, LipA, and LasB; no evidence of interactions was found with $Q_D$-$N^{012}$, $Q_D$-$N^{01}$, $T_G$, $X_K$, $U_H$, $V_I$, or $W_J$ under the stated experimental conditions.

Nonspecific binding was subtracted from the binding traces before calculation. Dissociation constants ($K_d$) were estimated based on the equilibrium levels at 100 and 50 s of injection of LasB and $Q_D$-$N^{0123}$, respectively. In Figs. 3 and 6–8, for all sensorgrams, the *inset* represents plots of equilibrium response levels ($\Delta RU$; *y* axis) as a function of analyte concentration ($\mu M$; *x* axis), with the curve fit to a 1:1 equilibrium model for determination of $K_D$ at 50% saturation response.

*Batch Co-purification (Pulldown) of $^{his}P_C$ and $Q_D$-$N^{0123}$, $Q_D$-$N^{012}$, and $Q_D$-$N^{01}$ and Quaternary Complex $U_H$-$V_I$-$W_J$-$X_K$ Periplasmic Domains*—Batch co-purification experiments were performed as described in Ref. 10. The exact experimental procedure is described in the supplemental material.

| Bound ligand | Analyte: Peri-$P_C$ | Peri-$Q_D$ | | | Pp body | Pp tip | | | | | Substrates (Xcp T2SS) | |
|---|---|---|---|---|---|---|---|---|---|---|---|---|
| | $P_C$ | $N^{0123}$ | $N^{012}$ | $N^{01}$ | $T_G$ | $U_HW_JV_IX_K$ | $U_H$ | $V_I$ | $W_J$ | $X_K$ | LasB | LipA |
| $^{his}P_C$ | - | 3.6 | - | - | - | - | - | - | - | - | 3.6 | 6.8 |
| LasB (Xcp T2SS) | 2.0 | 12.5 | 21.6 | 27.8 | - | 0.9 | 12.5 | 24.6 | - | 12.7 | ND | ND |
| LapA (Hxc T2SS) | - | - | - | - | - | - | - | - | - | - | ND | ND |

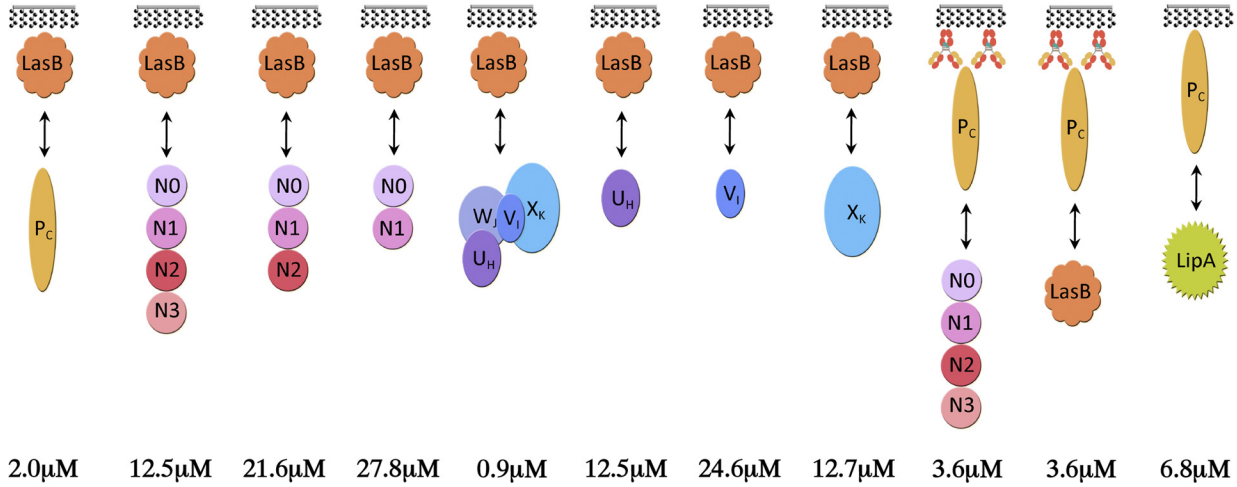


FIGURE 2. **Interaction network between the periplasmic domains of the *P. aeruginosa* Xcp secreton and substrates by SPR.** Ligand and analytes are indicated following the code used under "Experimental Procedures." Positive interactions are indicated by *black boxes*, in which the $K_d$ values (μM) of the interactions are indicated. *Gray boxes* with *dashes* indicate that no interaction was detected. The schemes for all positive interactions are represented below the table and follow the color code used in Fig. 1. *Pp*, pseudopilus; *ND*, not determined.

*Mass and Stoichiometry Calculation of XcpP-XcpQ Complex*—We characterized the mass of each soluble domain of $^{his}P_C$ and $Q_D$ using the combination of UV spectrophotometry, MALS, and refractometry, coupled on-line with an analytical size-exclusion chromatography column, and we determined the hydrodynamic radii using an online QELS. UV, MALS, QELS, and refractometry measurements were achieved with a photodiode array 2996 (Waters), a miniDAWN TREOS (Wyatt Technology), a DynaPro (Wyatt technology), and an Optilab rEX (Wyatt Technology), respectively. Mass and hydrodynamic radius calculations were performed the with the ASTRA software (Wyatt Technology) using a *dn/dc* value of 0.185 ml/g. The column used was a 15-ml KW-804 (Shodex) with at 0.25 ml $min^{-1}$ flow, on an Alliance HPLC 2695 system (Waters). The buffer was 50 mM Tris, pH 7.5, 150 mM NaCl. 50 μl (KW-804) of each protein sample at 5 mg/ml in Tris 50 mM, 150 mM NaCl, pH 7.5, were injected in each experiment. To estimate the stoichiometry of the complex, $P_C$-$Q_D$ $^{his}P_C$, and $Q_D$ were copurified using nickel affinity. Elution fractions were concentrated on Centricon with a 30-kDa cutoff and passed through a Sephadex 75 16/60 (GE Healthcare) equilibrated in 50 mM phosphate, 150 mM NaCl, pH 7. The Sephadex G75 was calibrated using the gel filtration LMW calibration kit (GE Healthcare). The ribonuclease A (13.7 kDa), ovalbumin (43 kDa) and conalbumin (75 kDa) were used as standard proteins to estimate the molecular mass of the $P_C$-$Q_D$ complex.

## RESULTS

*$XcpP_C$ Is the Peripheral Periplasmic Element of the Secreton*—$XcpP_C$ is a central constituent of the Xcp T2SS. This IM protein possesses a large periplasmic domain, which directly interacts with the OM component of the machinery, the secretin $XcpQ_D$ (16, 17) (Fig. 1*A*). To identify secretin domains as well as other secreton components that interact with the periplasmic part of $XcpP_C$, we systematically assayed *in vitro* interactions between the periplasmic soluble domains of $XcpP_C$ ($P_C$) and various periplasmic domains of secreton components. To this end, three variants of secretin soluble domains ($Q_D$) and the five pseudopilin soluble domains ($T_G$, $U_H$, $V_I$, $W_J$, and $X_K$) were engineered, produced, and purified in the mM range (see "Experimental Procedures"). Then, using two complementary techniques, affinity chromatography and SPR, we systematically tested *in vitro* protein/protein interactions using $^{his}P_C$. As expected, we confirmed the interaction between $P_C$ and $Q_D$ (Figs. 2 and 3, *A* and *B*). Moreover, to more precisely identify the $Q_D$ subdomains involved in this interaction, we constructed and tested two other truncated versions lacking N3 ($Q_D$-$N^{012}$) and the N3-N2 subdomain(s) ($Q_D$-$N^{01}$), in addition to the peri-

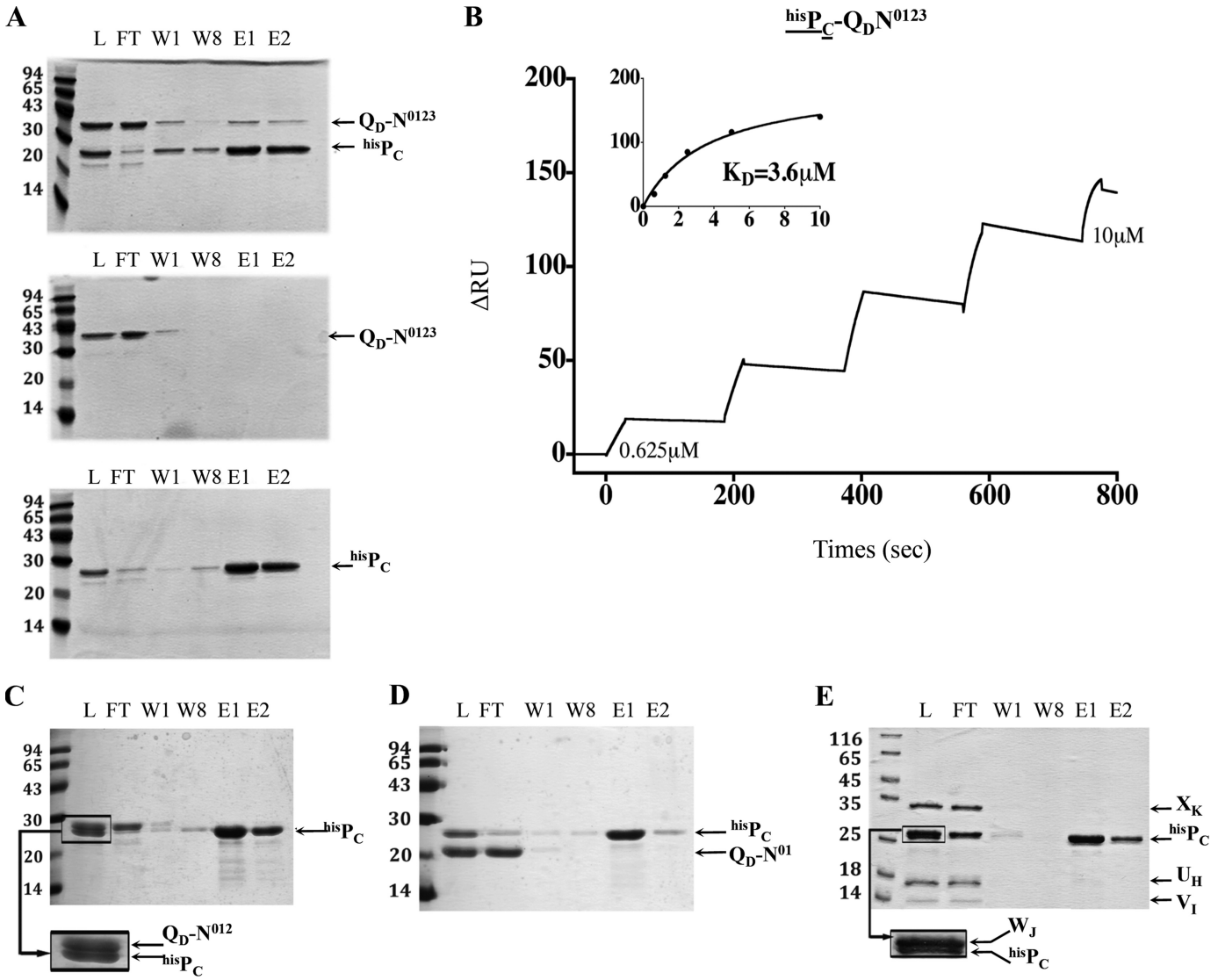


FIGURE 3. **$P_C$/$Q_D$ interaction identified by affinity chromatography and SPR experiments.** *A*, batch co-purification of $P_C$ and $Q_D$ presented in this panel were performed on affinity columns. $^{his}P_C$ and $Q_D$-$N^{0123}$ were mixed (*upper panel*) or loaded individually (*lower panels*) on an SDS-PAGE gel. *Fractions L*, *FT*, *W1*, *W8*, *E1*, and *E2*, respectively contain loaded protein, the flow-through, the washes, and the eluates. The positions of the molecular mass markers are indicated on the *left side* of each gel (kDa). *B*, the SPR sensorgram of the positive interaction found between $^{his}P_C$ (bound ligand, *underlined*) and $Q_D$-$N^{0123}$ (analyte) (see 'Experimental Procedures' for details). *C–E*, batch co-purification experiments of $^{his}P_C$ and $Q_D$-$N^{012}$ and $^{his}P_C$ and $Q_D$-$N^{01}$ and $^{his}P_C$ and of minor pseudopilin soluble domains $U_H$, $V_I$, $W_J$, and $X_K$, respectively, on affinity columns.

$XcpQ_D$-$N^{0123}$ ($Q_D$ or $Q_D$-$N^{0123}$). Both SPR and pulldown experiments indicated that the N3 subdomain of $Q_D$ was necessary for the interaction with $P_C$ because $Q_D$-$N^{012}$ lost its capacity to bind $P_C$ (Figs. 2 and 3, *C* and *D*). This result suggests that $P_C$ covers the whole periplasmic space; at one end, $XcpP_C$ is anchored into the IM, and at the other end, it interacts with N3, the closest OM secretin periplasmic subdomain (Fig. 1*A*) (15). Further experiments indicate that purified $P_C$ and $Q_D$ are monomeric in solution (Fig. 4*A*) and form a binary complex with a 1:1 ratio (Fig. 4, *B* and *C*). Based on recent cryo-electron microscopy data revealing an internal diameter of the dodecameric periplasmic secretin cavity of 55 Å (12), the binding of 12 $P_C$ inside the $Q_D$ cavity is structurally not feasible; therefore, it could only take place on the external face of the secretin pore. Consequently, we propose that 12 $P_C$ subunits form a dodecameric coat around the periplasmic portion of the secreton (see model in Fig. 1*A*).

Interestingly, we could not detect any interactions between $P_C$ and the pseudopilin soluble domains, either individually or as assembled in the quaternary pseudopilus tip complex, in either SPR or pulldown experiments (Figs. 2 and 3*E*). The absence of any interaction between $P_C$ and the pseudopilus components indicates that $P_C$ is physically separated from the pseudopilus. This result is in agreement with the secreton model, which presents the pseudopilus inside the secretin cavity (Fig. 1*A*) (15).

*Xcp Substrates First Interact with $XcpP_C$*—Three purified *P. aeruginosa* T2SS substrates, the elastase LasB, the lipase LipA, and the alkaline phosphatase LapA, were used in this study (Fig. 5). LasB is the most abundant protein secreted by the *P. aeruginosa* Xcp T2SS. The interaction between LasB and $P_C$ was analyzed by SPR. LasB was covalently immobilized on a CM5 chip, and SPR experiments revealed a specific interaction between LasB and $P_C$ (Figs. 1*B*, 2, and 6*A*). This newly described

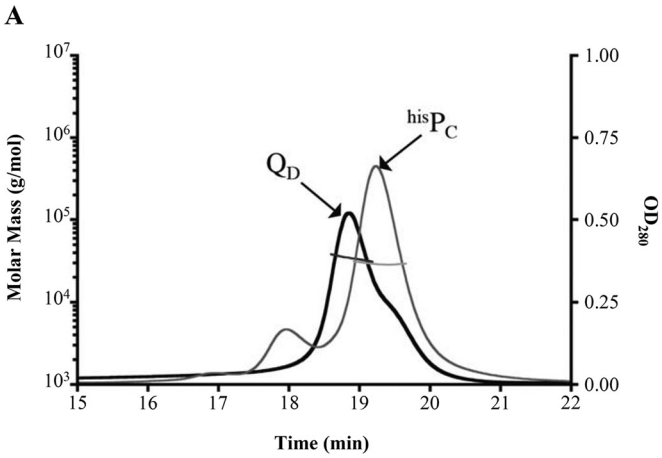


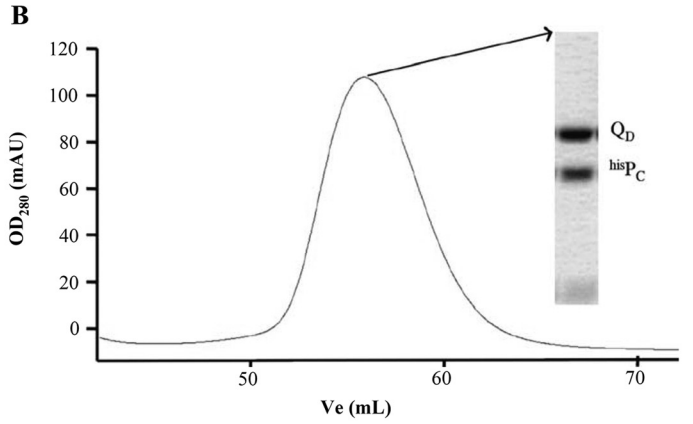


| Proteins | Theoretical MW (Da) | MW measured by WYATT (Da) | Rh |
|---|---|---|---|
| $^{his}P_C$ | 22,730 | 23,560 | 3.11 |
| $Q_D$ | 34,137 | 35,010 | 3 |

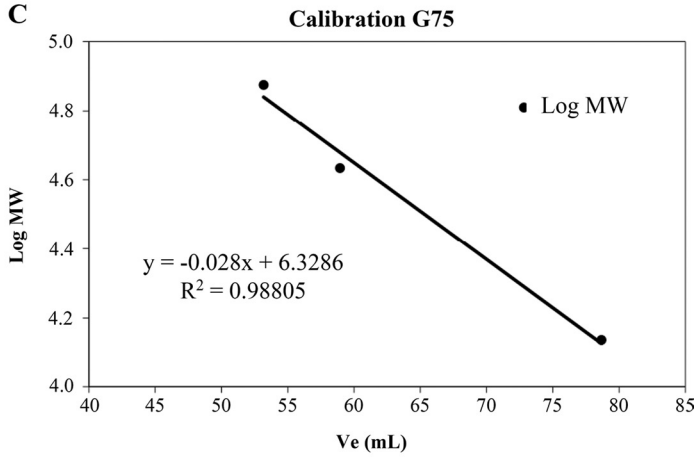


| Ve (mL) | Log MW | Estimated MW ($^{his}P_C$-$Q_D$) (kDa) | Calculated MW ($^{his}P_C$-$Q_D$) (kDa) |
|---|---|---|---|
| 56 | 4.7466 | 58.6 | 55.8 |

FIGURE 4. **Purified $P_C$ and $Q_D$ are monomeric in solution and interact in a 1:1 ratio.** *A*, $^{his}P_C$ and $Q_D$-$N^{0123}$ analyzed by MALS/QELS/UV/refractometry experiments. The protein masses of $^{his}P_C$ and $Q_D$-$N^{0123}$ were measured as 23,560 and 35,010 Da, respectively. These values are close to their respective theoretical masses of 22,730 and 34,137 Da obtained by ProtParam. *$OD_{280}$*, optical density at 280 nm. *B*, size-exclusion chromatography profile of the $^{his}P_C$-$Q_D$-$N^{0123}$ complex on a Sephadex 75 16/60 column. The *inset* represents an SDS-PAGE gel of the peak fraction, showing the $^{his}P_C$-$Q_D$-$N^{0123}$ complex. *mAU*, milliabsorbance units; *V*, elution volume. *C*, Sephadex 75 column calibration using gel filtration LMW standard proteins. The calculated mass of 55.8 kDa is in agreement with the estimated molecular mass of the $^{his}P_C$-$Q_D$-$N^{0123}$ complex by Wyatt Technology of 58.6 kDa.

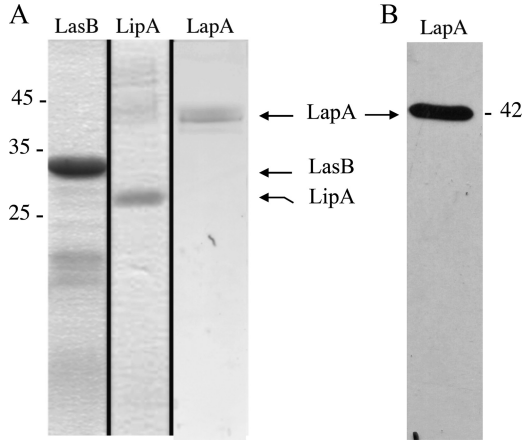


FIGURE 5. **Analysis of purified LasB, LipA, and LapA.** *A*, samples of purified LasB, LipA, and LapA used in SPR experiments were analyzed by 15% SDS-PAGE. After electrophoresis, the gel was stained with Coomassie Blue. The positions of the molecular mass markers (kDa) are indicated by a *dash*. The positions of purified LasB, LipA, and LapA are indicated by *arrows*. *B*, immunodetection of purified LapA with anti-LapA antibodies.

direct interaction between a substrate and one component of the secreton was confirmed by the reciprocal SPR experiment, in which $^{his}P_C$ was fixed to an anti-penta-His antibody covalently linked to a CM5 chip. Purified LasB was passed over $^{his}P_C$ and showed a significant affinity for it (Figs. 2 and 6*B*). The physiological relevance of such a $P_C$/substrate interaction during type II secretion is strengthened based on the positive interaction between $P_C$ and a second Xcp substrate, the lipase LipA (Figs. 2 and 6*C*). Furthermore, no interaction could be detected between $P_C$ and the alkaline phosphatase LapA, an exoprotein specifically secreted by the second *P. aeruginosa* T2SS system, Hxc (Fig. 2). This important result, which confirms the specificity of the interactions between $P_C$ and Xcp T2SS substrates, also validates the physiological relevance of our *in vitro* results. Considering that $XcpP_C$ forms the external wall of the periplasmic portion of the secreton, we propose that it is the first component of the secreton to bind the substrate, and therefore, that $XcpP_C$ is the recruiter of the system (Fig. 1*B*).

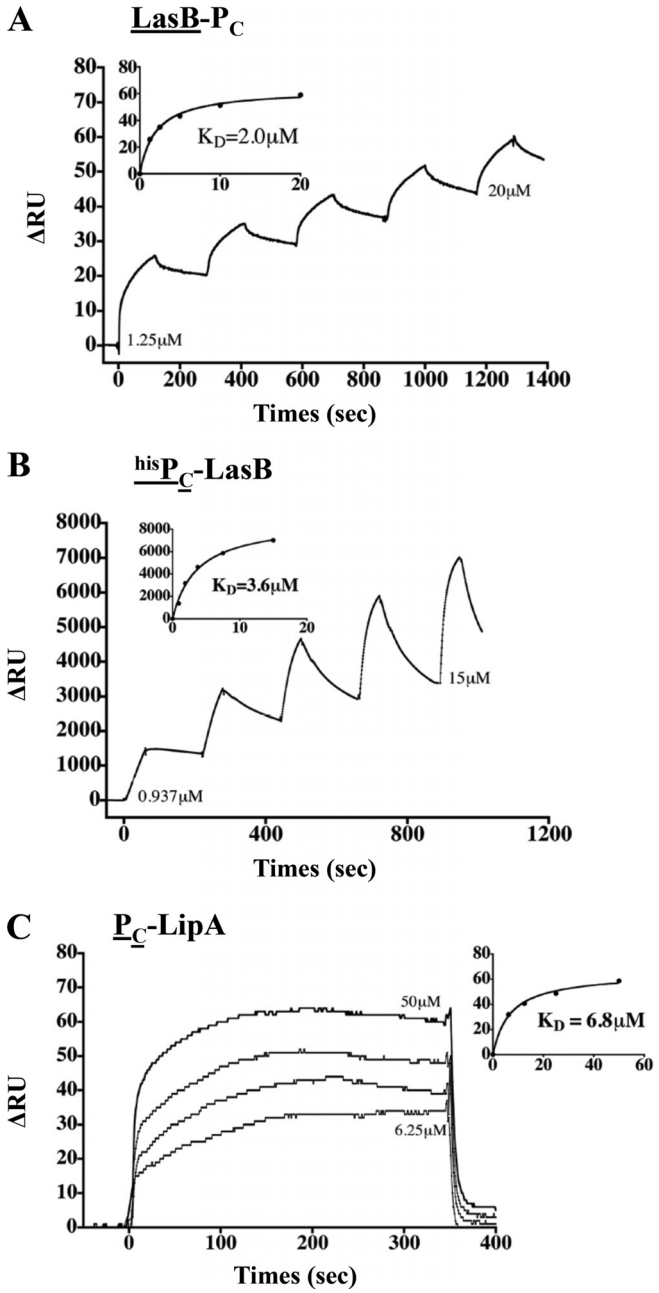


FIGURE 6. **P$_C$/substrate interactions identified by SPR.** *A–C*, the SPR sensorgrams of the positive interactions found between LasB and P$_C$, $^{his}$P$_C$ and LasB, and $^{his}$P$_C$ and LipA, respectively (see 'Experimental Procedures' for details). For each interaction experiment, the bound ligand is *underlined*.

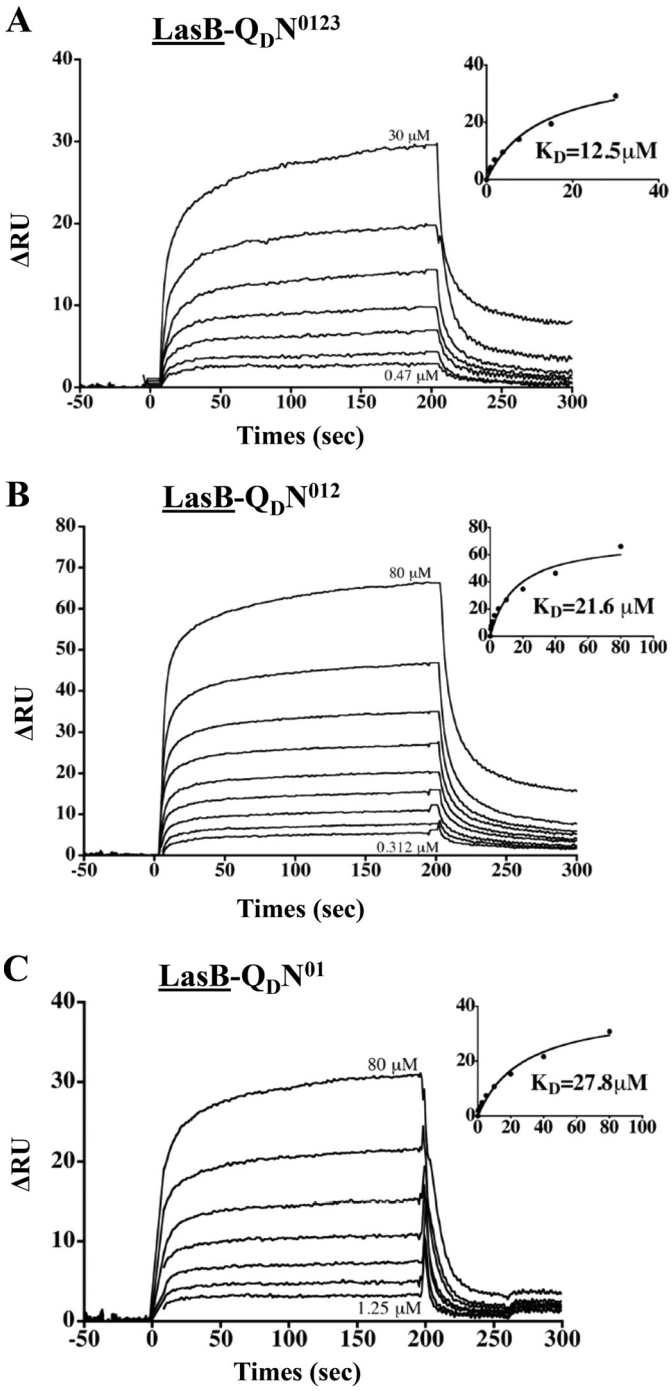


FIGURE 7. **LasB/Q$_D$ interactions identified by SPR.** *A–C*, the SPR sensorgrams of the positive interactions found between LasB (bound ligand, *underlined*) and Q$_D$-N$^{0123}$, Q$_D$-N$^{012}$, and Q$_D$-N$^{01}$, respectively (see 'Experimental Procedures' for details).

*LasB Binds the N0N1 Secretin Subdomains*—Once recruited by XcpP$_C$, the substrate is probably imported inside the machinery, where it should interact with several secreton components. One of these components is likely the partner of XcpP$_C$: the periplasmic soluble domain of the secretin. Using LasB covalently linked to a CM5 chip, we employed SPR to analyze the interactions between substrate and the four different periplasmic subdomains of the OM secretin. We passed Q$_D$-N$^{0123}$, Q$_D$-N$^{012}$, and Q$_D$-N$^{01}$ over LasB and found similar affinities for the three Q$_D$ subdomains, indicating that the LasB-interacting domain on Q$_D$ belongs to the two N0N1 subdomains (Figs. 1*C*, 2, and 7). This result, together with the previously identified interaction of P$_C$ with Q$_D$ through the N3 subdomain, indicates that two different interaction sites exist on Q$_D$: one for P$_C$ and another for LasB (Fig. 1, *A* and *C*). Moreover and in line with the substrate specificity, no interaction was detected between secretin subdomains and the Hxc-T2SS substrate LapA (Fig. 2).

*LasB Interacts with the Pseudopilus Tip*—Interaction with the secretin does not explain how the substrate could be released by the machinery. It could be hypothesized that inter-

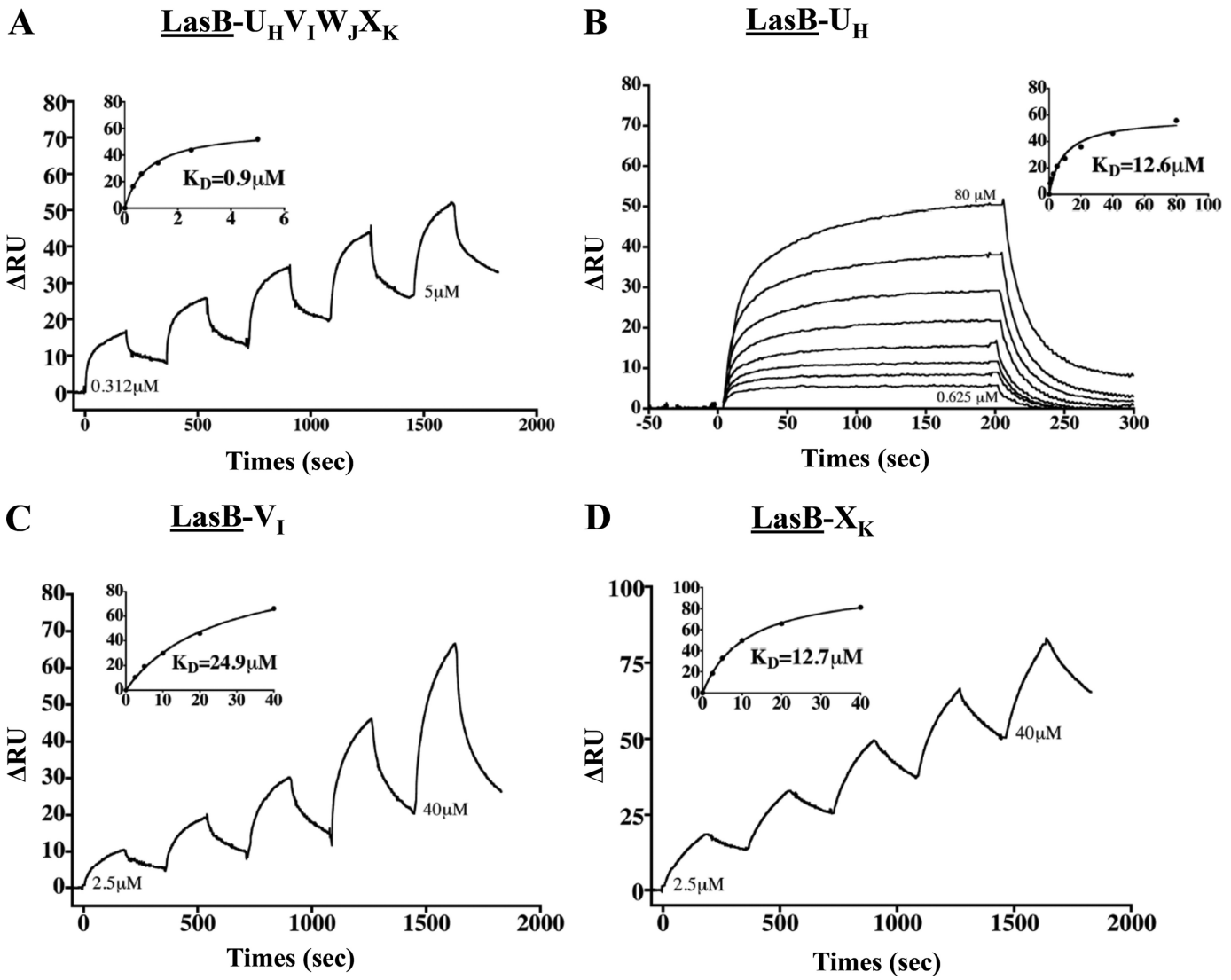


FIGURE 8. **LasB/pseudopilin interactions identified by SPR.** *A–D*, the SPR sensorgrams of the positive interactions found between LasB (bound ligand, *underlined*) and the $U_H$-$V_I$-$W_J$-$X_K$ complex, $U_H$, $V_I$, and $X_K$, respectively (see "Experimental Procedures" for details).

action with the secretin presents the substrate for expulsion by the growing pseudopilus. Using LasB immobilized on a CM5 chip, we measured its affinity for the five pseudopilins, either in a complex or individually. Our data revealed a direct interaction between the substrate and the quaternary complex of minor pseudopilins located at the tip of the pseudopilus (Figs. 1*D*, 2, and 8). Individual interactions between pseudopilins and LasB indicated that three of the four minor pseudopilin soluble domains, $U_H$, $V_I$, and $X_K$, interacted with the substrate, whereas $W_J$ did not show any significant binding (Figs. 2 and 8). Together with the recent SPR-identified interaction between the pseudopilus tip and the periplasmic domain of the secretin (12), our findings validate the piston model, in which the substrate, located in the secretin vestibule, is expelled out of the cell by the growing pseudopilus through the secretin pore.

Interestingly, no interaction was established between the substrate and the major pseudopilin soluble domain, $T_G$ (Fig. 2), suggesting that only the tip, and not the pseudopilus body, binds the substrate during the secretion process. This finding is in agreement with previous findings indicating that major pseudopilins could be exchanged among T2SSs without affecting their substrate specificity (23). It is noteworthy that no binding of any Xcp pseudopilins was observed when LapA was immobilized on the chip (Fig. 2).

## DISCUSSION

In the actual representation of the T2SS, the OM secretin is linked to the IM platform via its interaction with $GspC_P$, and the pseudopilus acts as a piston to push the substrate out through the secretin pore (4, 15, 24–28). This model, and more particularly the substrate recognition and transport mechanism, was very speculative because no interactions between the substrates and the components of the T2SS other than the secretin have been reported. In this study, we used SPR to identify several unprecedented specific interactions between secreted substrates and secreton components in the *P. aeruginosa* Xcp T2SS. For all of the substrate/secreton interactions tested, the estimated $K_d$ values were found in the micromolar range (Fig. 2). Such weak interactions suggest a transient stay of the substrate in the secreton during the secretion process.

All together, our results allowed us to propose a sequential model for substrate recognition and secretion by the T2SS (Fig. 1). In this model, we show that $XcpP_C$ bridges the inner and outer membrane elements of the machinery and probably envelopes the whole periplasmic part of the secreton (Fig. 1*A*). Thanks to the multiple specific interactions found between secreted substrates and secreton components, we propose that the exported exoproteins: (i) are initially recruited in the periplasm by the $XcpP_C$ (Fig. 1*B*), (ii) move into the periplasmic vestibule of the secretin (Fig. 1*C*), and (iii) are further pushed through the pore by the pseudopilus elongating from the IM platform (Fig. 1*D*). Finally, (iv) the pseudopilus retracts, allowing the positioning of a new substrate in the secretin vestibule for the next secretion cycle.

Two independent studies (16, 17) have shown that $GspC_P$ interacts with $GspD_Q$. Although none of these studies exclude the involvement of the $GspD_Q$ N3 subdomain, they clearly show that other $GspD_Q$ subdomains interact with $GspC_P$. In our case, $Q_D$-$N^{012}$ is incapable of binding $P_C$, whereas it is capable of binding substrates. This discrepancy could be due to subtle mechanistic differences between T2SSs, reflected by the low homology among $GspC_P$ components. On the $GspC_P$ side, Korotkov *et al.* (16) and Login *et al.* (17) agreed that $GspC_P$ bound $GspD_Q$ through one specific domain, the homology region (HR) (29). Notably, the $XcpP_C$ HR is not involved in substrate binding, according to Gerard-Vincent *et al.* (29), who showed that an $XcpP_C$ variant harboring the HR of the *Erwinia chrysanthemi* $OutC_P$ homolog was still able to secrete LasB from *P. aeruginosa*. In the same study, it was shown that an $XcpP_C$ variant containing the *Erwinia* $OutC_P$ TMHR located just upstream of the HR was non-functional, thus suggesting that specific substrate recognition by $GspC_P$ might implicate the TMHR. Interestingly, the TMHR is located right after the $XcpP_C$ transmembrane domain. We therefore suggest that newly periplasmic exported substrates might enter the secreton from its periplasmic base because they successively interact with $XcpP_C$ and N0N1 secretin subdomains located in the vicinity of the inner membrane.

The specific direct interactions identified between folded exoproteins and the five Xcp components provide important information about machinery/substrate recognition. Our findings indeed suggest that the secretion signal is located on the fully active native protein and not on an intermediate state of folding nor on a dedicated periplasmic chaperone, notably the elastase propeptide and the lipase foldase (4). Our data also confirm the conformational nature of the secretion signal because there are no common linear motifs on the 13 mature Xcp secreted proteins. Future studies will try to identify the LasB and LipA motif(s) specifically involved in their recruitment by $XcpP_C$ and subsequent interactions with the secretin and the pseudopilus.

In our secretion model, stoichiometric data presented in Fig. 4 indicate that 12 molecules of $XcpP_C$ surround the periplasmic portion of the secreton through 12 $P_C/Q_D$ heterodimeric interactions (Fig. 1*A*). This organization suggests that the secreton component initially contacted by the secreted proteins is $XcpP_C$. We found support for this hypothesis by identifying a direct interaction between $XcpP_C$ and two secreted proteins. Such a function for $XcpP_C$ in substrate recruitment and substrate specificity is in agreement with the low level of conservation among $GspC_P$ homologs in type II secretion machineries.

In our model, we propose that after recruitment by $XcpP_C$, the substrate first enters into the secretin vestibule in a position that allows it to be subsequently pushed by the pseudopilus growing from the IM platform. Notably, the binding of substrate to the pseudopilus prior to the secretin is unlikely because substrate has been visualized inside the secretin vestibule in the absence of the pseudopilus (30).

In conclusion, we identified in this study subtle, specific, and likely transitory interactions between T2SS-secreted exoproteins and the transport machinery. Collectively, our results provide an improved understanding of two important steps of the secretion process: substrate recognition and transport by the machinery. We propose an improved model of the type II secretion process, opening new routes for academic investigation and for antimicrobial targeting utilizing organic disruptors (31).

*Acknowledgments—We thank Christophe Quétard (GE Healthcare) for careful advice on SPR experiments, Sawsan Amara for assistance in lipase activity assays, Sophie Bleves, Alain Filloux, Katrina Forest, and Tâm Mignot for important and valuable discussions, and Yves-Michel Cully for preparation of Fig. 1.*

## REFERENCES

1. Economou, A., Christie, P. J., Fernandez, R. C., Palmer, T., Plano, G. V., and Pugsley, A. P. (2006) *Mol. Microbiol.* **62,** 308–319
2. Cianciotto, N. P. (2005) *Trends Microbiol.* **13,** 581–588
3. Voulhoux, R., Ball, G., Ize, B., Vasil, M. L., Lazdunski, A., Wu, L. F., and Filloux, A. (2001) *EMBO J.* **20,** 6735–6741
4. Filloux, A. (2004) *Biochim. Biophys. Acta* **1694,** 163–179
5. Patrick, M., Korotkov, K. V., Hol, W. G., and Sandkvist, M. (2011) *J. Biol. Chem.* **286,** 10378–10386
6. Py, B., Loiseau, L., and Barras, F. (2001) *EMBO Rep.* **2,** 244–248
7. Chen, Y., Shiue, S. J., Huang, C. W., Chang, J. L., Chien, Y. L., Hu, N. T., and Chan, N. L. (2005) *J. Biol. Chem.* **280,** 42356–42363
8. Abendroth, J., Bagdasarian, M., Sandkvist, M., and Hol, W. G. (2004) *J. Mol. Biol.* **344,** 619–633
9. Campos, M., Nilges, M., Cisneros, D. A., and Francetic, O. (2010) *Proc. Natl. Acad. Sci. U.S.A.* **107,** 13081–13086
10. Douzi, B., Durand, E., Bernard, C., Alphonse, S., Cambillau, C., Filloux, A., Tegoni, M., and Voulhoux, R. (2009) *J. Biol. Chem.* **284,** 34580–34589
11. Korotkov, K. V., and Hol, W. G. (2008) *Nat. Struct. Mol. Biol.* **15,** 462–468
12. Reichow, S. L., Korotkov, K. V., Hol, W. G., and Gonen, T. (2010) *Nat. Struct. Mol. Biol.* **17,** 1226–1232
13. Sauvonnet, N., Gounon, P., and Pugsley, A. P. (2000) *J. Bacteriol.* **182,** 848–854
14. Hu, N. T., Leu, W. M., Lee, M. S., Chen, A., Chen, S. C., Song, Y. L., and Chen, L. Y. (2002) *Biochem. J.* **365,** 205–211
15. Korotkov, K. V., Gonen, T., and Hol, W. G. (2011) *Trends Biochem. Sci.* **36,** 433–443
16. Korotkov, K. V., Krumm, B., Bagdasarian, M., and Hol, W. G. (2006) *J. Mol. Biol.* **363,** 311–321
17. Login, F. H., Fries, M., Wang, X., Pickersgill, R. W., and Shevchik, V. E. (2010) *Mol. Microbiol.* **76,** 944–955
18. Ball, G., Durand, E., Lazdunski, A., and Filloux, A. (2002) *Mol. Microbiol.* **43,** 475–485
19. Voulhoux, R., Taupiac, M. P., Czjzek, M., Beaumelle, B., and Filloux, A. (2000) *J. Bacteriol.* **182,** 4051–4058
20. Sauvonnet, N., and Pugsley, A. P. (1996) *Mol. Microbiol.* **22,** 1–7

21. Stuer, W., Jaeger, K. E., and Winkler, U. K. (1986) *J. Bacteriol.* **168,** 1070–1074
22. Rich, R. L., Hoth, L. R., Geoghegan, K. F., Brown, T. A., LeMotte, P. K., Simons, S. P., Hensley, P., and Myszka, D. G. (2002) *Proc. Natl. Acad. Sci. U.S.A.* **99,** 8562–8567
23. Vignon, G., Köhler, R., Larquet, E., Giroux, S., Prévost, M. C., Roux, P., and Pugsley, A. P. (2003) *J. Bacteriol.* **185,** 3416–3428
24. Filloux, A., Michel, G., and Bally, M. (1998) *FEMS Microbiol. Rev.* **22,** 177–198
25. Nunn, D. (1999) *Trends Cell Biol.* **9,** 402–408
26. Sandkvist, M. (2001) *Mol. Microbiol.* **40,** 271–283
27. Johnson, T. L., Abendroth, J., Hol, W. G., and Sandkvist, M. (2006) *FEMS Microbiol. Lett.* **255,** 175–186
28. Cianciotto, N. P. (2009) *Future Microbiol.* **4,** 797–805
29. Gérard-Vincent, M., Robert, V., Ball, G., Bleves, S., Michel, G. P., Lazdunski, A., and Filloux, A. (2002) *Mol. Microbiol.* **44,** 1651–1665
30. Reichow, S. L., Korotkov, K. V., Gonen, M., Sun, J., Delarosa, J. R., Hol, W. G., and Gonen, T. (2011) *Channels* **5,** 215–218
31. Shahian, T., Lee, G. M., Lazic, A., Arnold, L. A., Velusamy, P., Roels, C. M., Guy, R. K., and Craik, C. S. (2009) *Nat. Chem. Biol.* **5,** 640–646